Evaluation of the high temperature performance of HfB2 UHTC particulate filled Cf/C composites

Paul, Anish; Rubio Diaz, Virtudes; Binner, Jon; Vaidhyanathan, Bala; Heaton, Andrew; Brown, Peter

DOI:
10.1111/ijac.12659

Document Version
Early version, also known as pre-print

Citation for published version (Harvard):
Paul, A, Rubio Diaz, V, Binner, J, Vaidhyanathan, B, Heaton, A & Brown, P 2017, 'Evaluation of the high temperature performance of HfB2 UHTC particulate filled Cf/C composites', *International Journal of Applied Ceramic Technology*, vol. 14, no. 3, pp. 344-353. https://doi.org/10.1111/ijac.12659

International Journal of Applied Ceramic Technology
Ceramic Product Development and Commercialization

Evaluation of the High Temperature Performance of Cf-HfB_2 UHTC Composites

Journal:	*International Journal of Applied Ceramic Technology*
Manuscript ID	ACT-3687
Manuscript Type:	Article
Date Submitted by the Author:	29-Mar-2016
Complete List of Authors:	Paul, Anish; University of Birmingham, School of Metallurgy and Materials Binner, Jon; University of Birmingham, College of Engineering & Physical Sciences; University of Birmingham, Vaidhyanathan, Bala; Loughborough University, Materials Heaton, Andrew; Dstl, Brown, Peter; Dstl,
Keywords:	borides, ceramic matrix composites, oxidation resistance

Evaluation of the High Temperature Performance of Cf-HfB_2 UHTC Composites

A. Paul[a,1], J.G.P Binner[a], B.Vaidhyanathan[b], A.C.J. Heaton[c] and P.M. Brown[c]

[a]School of Metallurgy and Materials, University of Birmingham, Edgbaston, UK, B15 2TT

[b]Department of Materials, Loughborough University, UK, LE11 3TU

[c]Dstl, Porton Down, Salisbury, UK, SP4 0JQ

Abstract

Room and high temperature flexural strength and CTE of Cf-HfB_2 ultra-high temperature ceramic (UHTC) composites is determined along with UHT oxidation behaviour. Both room and high temperature strength of the composites were found to be broadly comparable to those of other thermal protection system materials currently being investigated. The CTE of the composites was measured both along and perpendicular to the fibre direction up to 1700°C and the values were found to depend on fibre orientation by approximately a factor of 3. Arc-jet testing of the UHTC composites highlighted the excellent ultra-high temperature oxidation performance of these materials.

[1]Now at Ansaldo Energia Switzerland AG.

Introduction

Ultra-high temperature ceramics (UHTCs) are candidate materials for use as leading edges, control surfaces, engine inlets and exits and engine hot flow path components in hypersonic vehicles. In recent years, these materials have been extensively investigated as innovative thermal protection systems (TPS)[1-3] and sharp leading edge components[4-6] for aerospace vehicles as well as for other applications where oxidation and/or erosion resistance at temperatures up to and exceeding 2000°C are required. The main materials that are being researched as UHTCs are the borides and carbides of transition metals, e.g. HfB_2, ZrB_2, HfC, and ZrC. They are refractory in nature and have melting temperatures above 3000°C.[7-9] The suitability of single phase ceramics is significantly limited, however, due to their poor thermal shock and oxidation resistance.[10] Even with the addition of a second or third ceramic phase, such as SiC or LaB_6, these materials do not possess the high temperature resistance, thermal shock resistance or fracture toughness required.[11]This clearly highlights the need to adopt a fibre reinforced composite approach. Carbon fibre (Cf) and silicon carbide fibre (SiCf) are two obvious choices, provided they can be protected at the application temperatures.

There are a number of reports in the literature about the preparation of continuous fibre reinforced UHTC composites using SiC[4, 12, 13] and C fibres.[14-30] Processing methodologies adopted for the preparation of UHTC composites include precursor infiltration and pyrolysis,[18-21] chemical vapour deposition,[22-24] reactive melt infiltration,[25, 26] slurry infiltration and pyrolysis[14-17] or a combination of processes.[27-29] A number of

groups dedicated their efforts to prepare short fibre reinforced composites,[30-35] the advantage being the ability to apply the processing techniques developed for monolithic UHTC materials. The improvement in mechanical properties, especially toughness, achieved with the latter class of materials was not significant, however.

Previous studies conducted by the present authors[16] compared the high temperature oxidation performance of a variety of Cf-based UHTC composites viz., Cf-ZrB_2, Cf-ZrB_2-20 vol%SiC, Cf-ZrB_2-20 vol%SiC-10 vol% LaB_6, Cf-HfB_2 and Cf-HfC, using an oxyacetylene flame and reported that the best performance was observed for Cf-HfB_2. The main focus of the present study was to determine the room and high temperature flexural strength of these UHTC composites together with the coefficient of thermal expansion (CTE) along and across the fibre direction. Ultra-high temperature oxidation tests were carried out using an arc-jet facility, which is considered as the best ground based testing technique for evaluating high temperature oxidation performance. Arc-jets provide conditions that are similar to the aero-thermal environment experienced during flight and hence the results are used to understand the thermal performance of materials and systems under controlled aero-thermal heating conditions. The results have been used to validate the numerical models of materials and systems that are used as design tools.[5] Nevertheless, there are a number of differences between arc-jet and flight environments that must be accounted for when interpreting the data. For example, surface catalycity can play a more significant role during arc-jet testing than in re-entry, because a higher proportion of the air molecules are dissociated in the former environment.[36] Detailed microstructural characterisation was carried out on the post

test samples and conclusions drawn about the advantages of incorporating UHTC particles on high temperature performance.

Experimental

Preparation of UHTC composites

The UHTC composites used in the current study were prepared utilizing a slurry composed of HfB_2 (325 mesh, HC Starck, Karlsruhe, Germany), acetone and phenolic resin (Cellobond J2027L, Hexion Specialty Chemicals, B. V., Rotterdam, The Netherlands). The ingredients were mixed in the required ratio, a typical formulation contained 40 g HfB_2, 20 g phenolic resin and 12.5 g acetone, and ball milled for 48 h to achieve a slurry with the required consistency (~10 mPa s at 100 s^{-1} shear rate). 2.5 D Cf preforms were obtained from Surface Transforms (Surface Transforms plc., Cheshire, UK). 180 x 30 x 15 mm Cf preforms were used for preparing UHTC composites for flexural strength and CTE measurements. 52 mm diameter by ~20 mm thick preforms was used for arc-jet samples. Impregnation of the preforms was carried out using a vacuum assisted technique where the preform was fully submerged in the UHTC slurry contained in a vacuum chamber. The chamber was then evacuated with a vacuum pump to facilitate the impregnation of the slurry. Further details on the composite processing can be found elsewhere.[16] Final densification was achieved using 5 cycles of chemical vapour infiltration (CVI) of carbon at Surface Transforms plc., Cheshire, UK. After CVI densification, flexural strength (140 x 25 x 10 mm) and CTE (10 x 5 x 5 mm) specimens were machined out from the larger composites. CTE specimens

were machined such that measurements could be made both along and perpendicular to the fibre direction. Arc-jet specimens were machined down to final dimensions of 30 mm diameter x 5 mm thickness so that they could be mounted in a carbon-carbon (CC) composite sample holder. CC composites for comparative measurements were prepared by CVI densification of 2.5D carbon fibre preforms at Surface Transforms, without any powder impregnation. The bulk density of Cf-HfB_2 and CC composites were 2.2 ± 0.14 and 1.8 ± 0.04 g cm^{-3} respectively. The final porosity of all the composites was around 10%.

Flexural strength and CTE measurements

Room temperature (RT) and high-temperature (HT) 4-point flexural strength measurements were carried out at CERAM [2] (Stoke-on-Trent, Staffordshire, UK) according to CERAM R102, method 2. RT strength measurements were conducted in air whereas HT strength measurements were carried out under a flowing argon atmosphere. The strength of the composites was determined using large, 140 x 25 x 10 mm, samples; this was essential to give a true representation of the UHTC composite because of its graded structure. As per the specification, prior to HT testing, the composites were coated with a commercial product known as Tipp-Ex (a slurry of TiO_2 in an organic medium intended for use as a paper correction fluid) all over the surface, except where it came in contact with the loading and support rollers, to minimise any oxidation due to the presence of residual oxygen. A 5N preload was applied to ensure proper contact between the sample and the rollers. The test rig used for HT testing,

[2] Now Lucideon Ltd

along with a Tipp-Ex coated test bar, is shown in Figure 1. The HT test parameters are summarised in Table 1. RT test parameters were similar except the fact that there was no heating or gas flow.

The argon flow rate employed was sufficient, in theory, to replace the atmosphere within the box furnace approximately 4 times every minute; this involved a flow rate of 15 L min^{-1}. Presence of residual oxygen is expected as the furnace employed is not a sealed system. The hold duration at 1400°C was limited to 5 min to minimise any oxidation at high temperature due to the presence of residual oxygen.

The CTE was measured at Imperial College London, UK, using a Netzsch 402C dilatometer (Netzsch-Geratebau GmbH, Selb, Germany) with a graphite sample holder and push rod. Samples were heated at 10°C min^{-1} from room temperature to 1700°C under helium atmosphere whilst recording the displacement of the pushrod. By calibrating the expansion of the set-up with a graphite sample of known thermal expansion, the displacement of the push-rod was converted in actual thermal expansion data for the sample. Since the pushrod exerted a force of ~1.5 N on the sample to ensure that good contact was maintained, data collected at the highest temperatures should be treated with caution as compressive creep might have counter-acted the thermal expansion of the sample.Specimens were prepared so that the CTE values could be measured both along and across the fibre directions

It is customary to describe the thermal expansion using eqn 1.

$$\frac{L(T)-L(T_{ref})}{L(T_{ref})}=\alpha_{avg}\cdot\Delta T \quad (1)$$

Where

α_{avg} - Average coefficient of thermal expansion from T_{ref} to T

L(T) – Length of sample at temperature T

$L(T_{ref})$ – Length of sample at reference temperature T_{ref}

$\Delta T = T - T_{ref}$

Arc-jet testing

Arc-jet tests of the samples were carried out at the German Aerospace Centre (Deutsches Zentrum fur Lüft- und Raumfahrt, DLR, Cologne, Germany). One UHTC sample (AJ5-20) was tested at a heat flux of 5 MW m^{-2} for ~20 s whereas a second sample (AJ10-10) was tested at 10 MW m^{-2} for ~10 s. The test parameters are summarised in Table 2. . The front face temperature during testing was measured using a two colour pyrometer (Dr. Maurer QKTR1485, Dr. Georg Maurer GmbH – Optoelektronik, Germany) calibrated from 900-3000°C and a spectral pyrometer (Dr. Maurer KTR1485-Z, Dr. Georg Maurer GmbH – Optoelektronik, Germany), sensitive at 1 micron and calibrated between 900-3000°C.

The surface and cross sectional microstructures and chemical compositions of the arc-jet samples were studied using field emission gun scanning electron microscopy

(FEGSEM, Leo 1530VP, LEO, Elektronenskopie GmbH, Oberkochen, Germany) and energy dispersive spectroscopy (EDS, EDAX Inc., NJ, USA).

Results and Discussion

Flexural Strength Measurement

The stress-strain curves for the CC and UHTC composites after RT and HT testing are given in Figure 2 and Table 3 summarises the flexural strength data.The alumina rollers failed on at least three occasions during the HT testing, resulting in step changes in the stress-strain curves. This can be identified from the stress-strain plots of UHTC-HT5, CC-HT1 and CC-HT2. One of these samples (CC-HT1) was retested and it yielded a much lower strength of 85.01 MPa. All other composites deformed and did not show any sign of obvious failure. The Tipp-Ex applied on the surface formed a pale yellow substance, which was identified to be mainly TiO_2. A white layer on the surface of the UHTC composite after HT strength testing was characterised using EDS (data not shown) and found to be HfO_2. The oxidation of the Tipp-Ex and HfB_2 confirmed the presence of residual oxygen at the test temperature.

The CC composites displayed a higher deformation at room temperature compared to the UHTC composites. No brittle failure was observed at RT or HT, but rather a small amount of deformation was observed. CC composites were also coated with Tipp-EX prior to testing, but it fell off completely during the test, possibly due to the degradation of the surface carbon fibres. There was negligible mass change for the UHTC

composites after HT testing, but the CC composites had ~12% mass loss indicating oxidation of the test bars at elevated temperatures.

The average RT strength of UHTC composites was 111 ± 20 MPa and that of CC composites 132 ± 28 MPa. The average HT strength of UHTC composites was 103 ± 25 MPa and that of CC composites 126 ± 10 MPa. The RT strength values reported in the literature for UHTC composites include 107 MPa[19] or 150-170 MPa[12] for Cf-ZrC; 237 MPa for Cf/ZrB_2-SiC;[28] 25 MPa for Cf-HfC[22] and ~100 or 162 MPa for a functionally graded Cf/HfB_2-SiC composite[37] the latter values depending on whether the SiC or HfB_2 side was in tension. It is not accurate to make direct comparisons as the properties of a composite depends on the fibre volume fraction, fibre surface treatment, fibre orientation, amount of porosity, type of carbon deposit, processing temperature and the type and amount of fillers.

Considering the error bars, it is reasonable to conclude that there was no decrease in the average strength of the UHTC and CC composites at 1400°C, though it is difficult to make any statistical conclusions because of the failure of the rollers in some instances and the partial oxidation of the composites. CC composites showed a slightly higher strength compared to UHTC composites at both room and high temperature. This is not that surprising as the addition of UHTC powder was expected to reduce the overall strength of the composites by forcing apart the tows slightly as the UHTC powder penetrated.

The difficulties associated with the failure of the support rollers at high temperature along with a need for improved atmosphere control needs to be addressed in the future to improve the accuracy of measurements.

CTE Measurements

The change in length of the samples with temperature for the UHTC and CC composites from the initial heating is shown in Figure 3 a. All samples showed a largeexpansion around 1000°C, followed by shrinkage around 1250°C. In one case, the shrinkage was so strong that after cooling, a permanent shrinkage of about 50 μm on a 10 mm sample was recorded. As this variation was also observed for the CC samples it is assumed that the carbon fibres were allowing the CVI deposited carbon and/or HfB_2 powder to undergo some rearrangement at this temperature. It has been reported that for carbon materials, the thermal expansion in any direction is equal to the sum of crystallite expansions resolved in that direction but a proportion of that is accommodated by internal adjustments. The degree of accommodation is primarily dependent on the preferred orientation of the crystallites with a secondary dependence on the apparent density of carbon. The presence of sub-microscopic porosity is responsible for this secondary dependence; [37] the CC and UHTC composites in the present study had a porosity of around 10%. It is also worth noting that the rapid change in dimensions was observed above the temperature employed for CVI of carbon, the highest seen by the sample during processing, prior to CTE measurements. This also suggested that the processing temperature may not have been sufficient to produce materials that were stable at high temperatures. As a result of these variations, a

second round of measurements was also carried out for the same samples and the results are shown in Figure 3 b. This run produced rather smooth curves without much change in slope and the average CTE values from these measurements are summarised in Table 4.

The average CTE values of the UHTC composites were found to be 1.63 ± 0.13 x 10^{-6} $°C^{-1}$ and 4.67 ± 0.21 x 10^{-6} $°C^{-1}$ respectively along and across the ply. The corresponding values for the CC composites were 2.83 ± 0.09 x 10^{-6} $°C^{-1}$ and 4.24 ± 0.49 x 10^{-6} $°C^{-1}$ respectively. Type of fiber, type of matrix, bonding between the fiber and matrix, volume fraction of the fiber and inter-ply angle are all factors that could influence the CTE values. The CTE of Cf along the axis is reported to be negligible (~0 x 10^{-6} $°C^{-1}$) compared to the value in the radial direction (~8 x 10^{-6} $°C^{-1}$).[38] Polymer derived carbon has a CTE of 2 - 4 x 10^{-6} $°C^{-1}$ and pyrolytic carbon, which is isotropic, has a CTE value in the range 4 - 6 x 10^{-6} $°C^{-1}$.[39] The CTE of HfB_2 is reported to be 6.3 - 7.6 x 10^{-6} $°C^{-1}$.[36] So it can be assumed that the lower CTE of CC and UHTC composites along the ply are mainly due to the lower CTE of Cf along the axial direction. The contribution of each constituent phase to the final CTE can be estimated provided the mass fraction of each of the constituents, i.e. Cf, polymer derived carbon (from the phenolic resin), pyrolytic carbon (from CVI), HfB_2 and submicroscopic porosity are known along with the integrity of the bond between the fiber and matrix.

The variation in CTE values along and across the fiber direction needs careful consideration while designing TPS components using UHTC composites. This variation

can also be used as a design tool to fabricate UHTC composites with tailored CTE values.

Arc Jet testing of UHTC Composites

Figure 4 shows one of the Cf-HfB_2 samples being tested, whilst the time-temperature profiles during testing are given in Figure 5. Figure 6 compares the images of the composites before and after the test. AJ5-20 has seen a peak temperature of ~2500°C whereas the sample tested at the higher heat flux , AJ10-10 reached around 2700°C. Melting of the UHTC phase was not observed at 5 MW m^{-2}, whereas melting was observed at 10 MW m^{-2} indicating that the actual temperature experienced by the sample may have been higher than the measured value (melting point of HfO_2 ~2900°C).[40] The oxide layer formed on AJ5-20 was uniform whereas the higher velocity jet removed some of the molten materials from the surface of AJ10-10 during the test. Both samples survived the rapid heating and maintained their integrity indicating their ability to withstand ultra-high temperatures and thermal shocks. Combining this with their lower density, UHTC composites have an advantage over UHTC monoliths for UHT applications.

Figure 7 shows the surface microstructure of AJ5-20 after testing. The surface of the sample indicated the presence of defects, Figure 7 a. Necking of the particles was observed, as shown in Figure 7 b. Figure 7 c shows an area near the edge of the sample, where the surface layer became delaminated during the test. This delamination may have been caused by defects generated during the machining of the composite to the required dimensions, causing the fibres underneath the surface layer to be exposed

to the jet. The carbon fibres underwent severe degradation and the UHTC particles showed partial oxidation; they were not exposed to the jet for long enough to undergo complete oxidation, Figure 7 d. Similar partial oxidation behaviour was reported for TaC during high temperature testing.[41, 42]

AJ10-10 sample experienced a higher temperature and heat flux compared to AJ5-20, but the test duration was shorter. The oxide particles were melted and, on solidification, formed a dense layer as shown in Figure 8 a. Cracks were observed in this layer. The particles also formed a protective layer for the carbon fibres, Figure 8 b. An interesting observation made on the sample was the degradation and severe pitting of the carbon fibres near the edge of the composite, Figure 8 c. This type of damage is believed to be due to the chemical attack on the fibres by the highly reactive gaseous species in the jet, including monoatomic oxygen. A cross section of the sample revealed the thickness of the surface layer, which was found to be ~45 μm, Figure 8 d. The surface cracks observed in Figure 8 a were not propagated to the bulk of the composite, offering protection for the underlying carbon fibers.

Conclusions

The room and high temperature flexural strength and coefficient of thermal expansion of Cf-HfB_2 UHTC composites have been determined and compared with those of carbon-carbon composites. The CC composites showed a slightly higher strength than the UHTC composites at both room and high temperature, but the reduction in strength at 1400°C was relatively small, <10 MPa, for both groups. There are hardly any reports in the literature on the high temperature flexural strength of UHTC composites, but it can

be concluded that the high temperature flexural strength of the UHTC composites from the present study is comparable to those of current generation TPS materials at this temperature.

CTE measurements for the UHTC composites revealed a large variation along and across the ply. The CTE along the fibre direction is controlled by the CTE of the carbon fibre in the axial direction; whilst that perpendicular is controlled by the CTE of the polymer-derived carbon, pyrolytic carbon and UHTC particles.

The arc-jet test is the first of its kind reported for slurry impregnated UHTC composites. Although the test durations were short, the samples retained their shape and the surface erosion was minimal. The UHTC particles formed a protective layer at high temperature which was beneficial for the performance of the composite.

A combination of low density, good mechanical properties, defect and thermal shock resistance and high temperature oxidation resistance displayed by the Cf-HfB_2 UHTC composites from this study clearly highlighted their potential for hypersonic applications. It is necessary to carry out high temperature strength measurements under a completely inert atmosphere and at even higher temperatures (1700°C or higher) to develop a better understanding of these materials at their application temperature. It is also essential to conduct arc-jet testing for longer durations.

Acknowledgements

The authors thank the UK's Defence Science and Technology Laboratory (DSTL) for providing the financial support for this work under contract number DSTLX-1000015267.

Dr. Luc Vandeperre is thanked for his help with measuring CTE at Imperial College, London.

Figure Captions

Figure 1 4-point bend test rig at CERAM. A test bar coated with Tipp-Ex® can also be seen.

Figure 2 Stress-strain curves after flexural strength testing. (a) CC at RT, (b) CC at HT, (c) UHTC at RT and (d) UHTC at HT.

Figure 3 Change in length with temperature for CC and UHTC composites. (a) Initial run and (b) repeated run.

Figure 4 A picture of one of the samples being arc jet tested, showing the demanding nature of the test.

Figure 5 Time-temperature profile during the arc-jet testing of UHTC composites. (a) AJ5-20 and (b) AJ10-10.

Figure 6 UHTC composites before and after arc-jet testing. (a) AJ5-20 before test, (b) AJ5-20 after test, (c) AJ10-10 before test and (d) AJ10-10 after test.

Figure 7 Surface microstructure of AJ5-20 after arc-jet testing. (a) Surface of the sample, (b) higher magnification image showing necking of oxide particles, (c) is an area where the fibres were exposed to the jet and (d) is a higher magnification image of the highlighted area showing partial oxidation of UHTC particles.

Figure 8 Microstructure of AJ10-10 after arc-jet testing. (a) Microstructure formed by the melting of UHTC particles, (b) carbon fibre protected by the UHTC phase, (c) severe pitting of fibres near the edge of the composite and (d) a cross-section revealing the thickness of the surface layer.

References

1. M. M. Opeka, I. G. Talmy, and J. A. Zaykoski, "Oxidation-based materials selection for 2000°C + hypersonic aerosurfaces: Theoretical considerations and historical experience," *J. Mater. Sci.,* 39[19] 5887-904 (2004).

2. A. L. Chamberlain, W. G. Fahrenholtz, G. E. Hilmas, and D. T. Ellerby, "Characterization of zirconium diboride for thermal protection systems," *Key Eng. Mater.,* 264 493-96 (2004).

3. R. Savino, M. De Stefano Fumo, D. Paterna, and M. Serpico, "Aerothermodynamic study of UHTC-based thermal protection systems," *Aerosp. Sci. Technol.,* 9[2] 151-60 (2005).

4. S. R. Levine, E. J. Opila, M. C. Halbig, J. D. Kiser, M. Singh, and J. A. Salem, "Evaluation of ultra-high temperature ceramics for aeropropulsion use," *J. Eur. Ceram. Soc.,* 22[14-15] 2757-67 (2002).

5. M. Gasch, D. Ellerby, E. Irby, S. Beckman, M. Gusman, and S. Johnson, "Processing, properties and arc jet oxidation of hafnium diboride/silicon carbide ultra high temperature ceramics," *J. Mater. Sci.,* 39[19] 5925-37 (2004).

6. X. Zhang, P. Hu, J. Han, and S. Meng, "Ablation behavior of ZrB2–SiC ultra high temperature ceramics under simulated atmospheric re-entry conditions," *Composites Sci. Technol.,* 68[7-8] 1718-26 (2008).

7. E. Wuchina, E. Opila, M. Opeka, W. Fahrenholtz, and I. Talmy, "UHTCs: ultra-high temperature ceramic materials for extreme environment applications," *The Electrochemical Society Interface,* 16[4] 30 (2007).

8. F. Monteverde, A. Bellosi, and L. Scatteia, "Processing and properties of ultra-high temperature ceramics for space applications," *Mater. Sci. Eng., A,* 485[1] 415-21 (2008).

9. W. G. Fahrenholtz, G. E. Hilmas, I. G. Talmy, and J. A. Zaykoski, "Refractory Diborides of Zirconium and Hafnium," *J. Am. Ceram. Soc.,* 90[5] 1347-64 (2007).

10. I. G. Talmy, J. A. Zaykoski, and M. M. Opeka, "Synthesis, processing and properties of TaC–TaB2–C ceramics," *J. Eur. Ceram. Soc.,* 30[11] 2253-63 (2010).

11. J. Han, P. Hu, X. Zhang, S. Meng, and W. Han, "Oxidation-resistant ZrB2–SiC composites at 2200°C," *Composites Sci. Technol.,* 68[3-4] 799-806 (2008).

12. N. Padmavathi, K. Ray, J. Subrahmanyam, P. Ghosal, and K. Sweety, "New route to process uni-directional carbon fiber reinforced (SiC + ZrB2) matrix mini-composites," *J. Mater. Sci.,* 44[12] 3255-64 (2009).

13. C. J. Leslie, E. Boakye, K. A. Keller, and M. K. Cinibulk, "Development of continuous SiC fiber reinforced HfB2-SiC composites for aerospace applications," pp. 3-12. in Processing and propeties of advanced ceramics and composites V*,* Vol. 240**.** *Ceramic Transactions.* Edited by N. P. Bansal, J. P. Singh, S. W. Ko, R. H. R. Castro, G. Pickrell, N. J. Manjooran, K. M. Nair, and G. Singh. John Wiley&Sons, 2013.

14. S. Tang, J. Deng, S. Wang, W. Liu, and K. Yang, "Ablation behaviors of ultra-high temperature ceramic composites," *Mater. Sci. Eng., A,* 465[1-2] 1-7 (2007).

15. A. Paul, D. D. Jayaseelan, S. Venugopal, E. Zapata-Solvas, J. Binner, B. Vaidhyanathan, A. Heaton, P. Brown, and W. E. Lee, "UHTC composites for hypersonic applications," *Am. Ceram. Soc. Bull.,* 91 22-29 (2012).

16. A. Paul, S. Venugopal, J. G. P. Binner, B. Vaidhyanathan, A. C. J. Heaton, and P. M. Brown, "UHTC–carbon fibre composites: Preparation, oxyacetylene torch testing and characterisation," *J. Eur. Ceram. Soc.,* 33[2] 423-32 (2013).

17. D. D. Jayaseelan, R. G. de Sa, P. Brown, and W. E. Lee, "Reactive infiltration processing (RIP) of ultra high temperature ceramics (UHTC) into porous C/C composite tubes," *J. Eur. Ceram. Soc.,* 31[3] 361-68 (2011).

18. D. Zhao, C. Zhang, H. Hu, and Y. Zhang, "Ablation behavior and mechanism of 3D C/ZrC composite in oxyacetylene torch environment," *Composites Sci. Technol.,* 71[11] 1392-96 (2011).

19. D. Zhao, C. Zhang, H. Hu, and Y. Zhang, "Preparation and characterization of three-dimensional carbon fiber reinforced zirconium carbide composite by precursor infiltration and pyrolysis process," *Ceram. Int.,* 37[7] 2089-93 (2011).

20. Z. Wang, S. Dong, X. Zhang, H. Zhou, D. Wu, Q. Zhou, and D. Jiang, "Fabrication and properties of Cf/SiC-ZrC composites," *J. Am. Ceram. Soc.,* 91[10] 3434-36 (2008).

21. Q. Li, S. Dong, Z. Wang, P. He, H. Zhou, J. Yang, B. Wu, and J. Hu, "Fabrication and properties of 3-D Cf/SiC-ZrC composites, using ZrC precursor and polycarbosilane," *J. Am. Ceram. Soc.,* 95[4] 1216-19 (2012).

22. A. Sayir, "Carbon fiber reinforced hafnium carbide composite," *J. Mater. Sci.,* 39[19] 5995-6003 (2004).

23. M. C. L. Patterson, S. He, L. L. Fehrenbacher, J. Hanigofsky, and B. D. Reed, "Advanced HfC-TaC Oxidation Resistant Composite Rocket Thruster," *MMP,* 11[3] 367-79 (1996).

24. M. C. L. Patterson, "Oxidation resistant HfC-TaC rocket thruster for high performance propellants," pp. 1-24. in*,* Vol. NAS3-27272. 1999.

25. L. Zou, N. Wali, J.-M. Yang, and N. P. Bansal, "Microstructural development of a Cf/ZrC composite manufactured by reactive melt infiltration," *J. Eur. Ceram. Soc.,* 30[6] 1527-35 (2010).

26. Y. Zhu, S. Wang, W. Li, S. Zhang, and Z. Chen, "Preparation of carbon fiber-reinforced zirconium carbide matrix composites by reactive melt infiltration at relative low temperature," *Scripta Mater.,* 67[10] 822-25 (2012).

27. Y. Wang, W. Liu, L. Cheng, and L. Zhang, "Preparation and properties of 2D C/ZrB2-SiC ultra high temperature ceramic composites," *Special Topic Section: Probing strains and Dislocation Gradients with diffraction,* 524[1–2] 129-33 (2009).

28. L. Li, Y. Wang, L. Cheng, and L. Zhang, "Preparation and properties of 2D C/SiC–ZrB2–TaC composites," *Ceram. Int.,* 37[3] 891-96 (2011).

29. H. Hu, Q. Wang, Z. Chen, C. Zhang, Y. Zhang, and J. Wang, "Preparation and characterization of C/SiC–ZrB2 composites by precursor infiltration and pyrolysis process," *Ceram. Int.,* 36[3] 1011-16 (2010).

30. F. Yang, X. Zhang, J. Han, and S. Du, "Characterization of hot-pressed short carbon fiber reinforced ZrB2–SiC ultra-high temperature ceramic composites," *J. Alloys Compd.,* 472[1-2] 395-99 (2009).

31. C. Musa, R. Orrù, D. Sciti, L. Silvestroni, and G. Cao, "Synthesis, consolidation and characterization of monolithic and SiC whiskers reinforced HfB2 ceramics," *J. Eur. Ceram. Soc.,* 33[3] 603-14 (2013).

32. L. Silvestroni, D. Sciti, C. Melandri, and S. Guicciardi, "Toughened ZrB2-based ceramics through SiC whisker or SiC chopped fiber additions," *Special Issue: Aerospace Materials for Extreme Environments,* 30[11] 2155-64 (2010).

33. P. Zhang, P. Hu, X. Zhang, J. Han, and S. Meng, "Processing and characterization of ZrB2–SiCW ultra-high temperature ceramics," *J. Alloys Compd.,* 472[1–2] 358-62 (2009).

34. X. Zhang, L. Xu, S. Du, C. Liu, J. Han, and W. Han, "Spark plasma sintering and hot pressing of ZrB2–SiCW ultra-high temperature ceramics," *J. Alloys Compd.,* 466[1–2] 241-45 (2008).

35. X. Zhang, L. Xu, S. Du, J. Han, P. Hu, and W. Han, "Fabrication and mechanical properties of ZrB2–SiCw ceramic matrix composite," *Mater. Lett.,* 62[6–7] 1058-60 (2008).

36. M. Gasch, D. Ellerby, and S. Johnson, "Handbook of Ceramic Composites," pp. 197-224. Springer US, (2005).

37. S. R. Levine, E. J. Opila, R. C. Robinson, and J. A. Lorincz, "Characterization of an Ultra-High Temperature Ceramic Composite," pp. 1-26. in, Vol. NASA TM-2004-213085. NASA technical report, 2004.

38. R. A. J. Sambell, D. H. Bowen, and D. C. Phillips, "Carbon fibre composites with ceramic and glass matrices," *J. Mater. Sci.,* 7[6] 663-75 (1972).

39. R. I. Baxter, R. D. Rawlings, N. Iwashita, and Y. Sawada, "Effect of chemical vapor infiltration on erosion and thermal properties of porous carbon/carbon composite thermal insulation," *Carbon,* 38[3] 441-49 (2000).

40. R. Ruh, H. J. Garrett, R. F. Domagala, and N. M. Tallan, "The Systern zirconia-hafnia," *J. Am. Ceram. Soc.,* 51[1] 23-28 (1968).

41. E. L. Courtright, J. T. Prater, G. R. Holcomb, G. R. S. Pierre, and R. A. Rapp, "Oxidation of hafnium carbide and hafnium carbide with additions of tantalum and praseodymium," *Oxid. Met.,* 36[5/6] 423-37 (1991).

42. A. Paul, J. G. P. Binner, B. Vaidhyanathan, A. C. J. Heaton, and P. M. Brown, "Oxyacetylene torch testing and microstructural characterization of tantalum carbide," *J. Microsc.,* 250[2] 122-29 (2013).

List of Tables

Table 1 HT 4-point bend test parameters used at CERAM.

Parameter	Value
Test temperature / °C	1400
Heating rate / °C min^{-1}	50
Hold duration at 1400°C / min	5
Argon flow rate / L min^{-1}	15
Initial load / N	5
Cross head speed / mm min^{-1}	0.5
Support span / mm	80
Loading span / mm	40

Table 2 Arc-jet test parameters

Parameter	Value	
Sample	AJ5-20	AJ10-10
Test Duration / s	20.1	10.6
Heat flux / MW m^{-2}	5.1	10.1
Distance from the nozzle exit / mm	160	100
Peak measured temperature / °C	2400	2650
Specific gas enthalpy / MJ kg^{-1}	15.9	
Nozzle configuration	50 mm exit diameter	
Test gas or atmosphere	Air	

Table 3 RT and HT strength of UHTC and CC composites.

UHTC Composites				CC Composites			
RT		HT		RT		HT	
Sample	Max. Str / MPa	Sample	Max. Str / MPa	Sample	Max. Str / MPa	Sample	Max. Str / MPa
UHTC-RT1	139.69	UHTC-HT1	124.96	CC-RT1	142.70	CC-HT1	130.97*
UHTC-RT2	116.98	UHTC-HT2	124.10	CC-RT2	175.59	CC-HT2	108.64*
UHTC-RT3	111.84	UHTC-HT3	119.32	CC-RT3	86.97	CC-HT3	120.88
UHTC-RT4	75.23	UHTC-HT4	85.51	CC-RT4	126.41	CC-HT4	131.26
UHTC-RT5	113.54	UHTC-HT5	62.67*	CC-RT5	129.15	CC-HT5	139.45

(* Indicates the failure of the alumina rollers during testing)

Table 4 CTE values of CC and UHTC composites.

Material	**α_{avg} x 10^6 °C^{-1} (25 – 1700°C)**
Cf-HfB_2 along the ply	1.63 ± 0.13
Cf-HfB_2 across the ply	4.67 ± 0.21
CC along the ply	2.83 ± 0.09
CC across the ply	4.24 ± 0.49

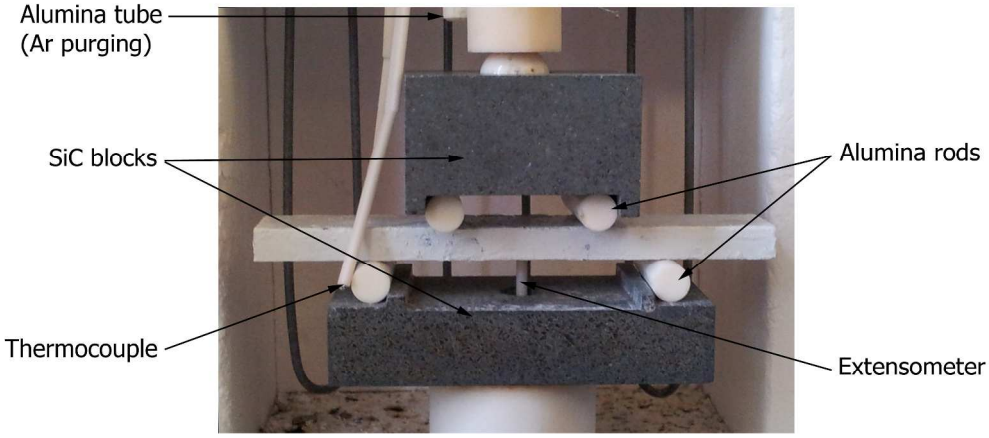

Fig 1 4-point bend test rig at CERAM. A test bar coated with Tipp-Ex® can also be seen
260x139mm (300 x 300 DPI)

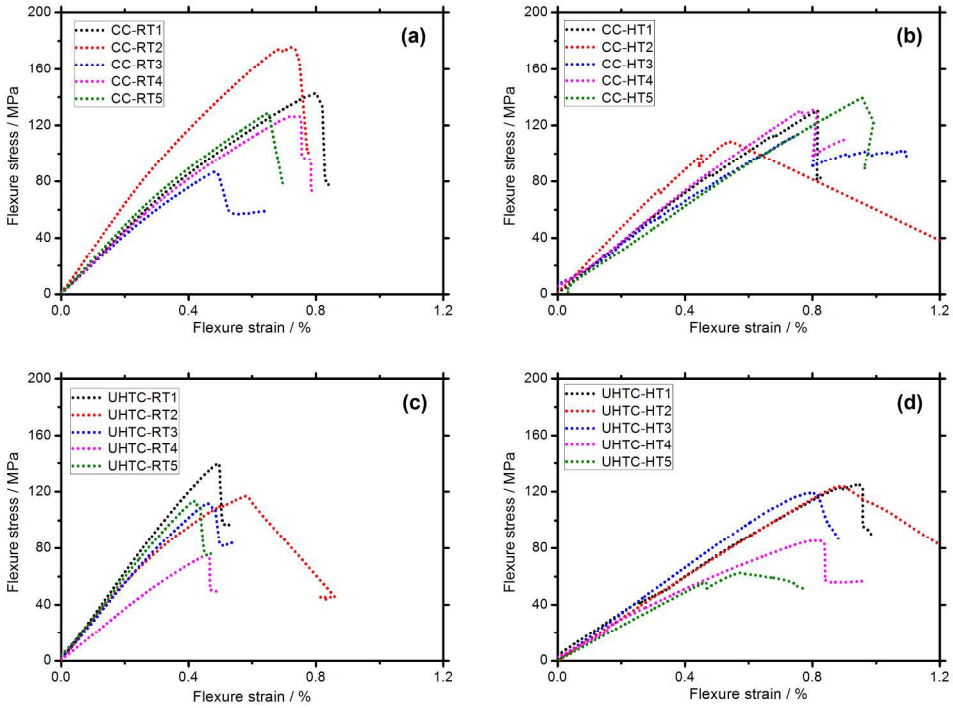

Fig 2 Stress-strain curves after flexural strength testing. (a) CC at RT, (b) CC at HT, (c) UHTC at RT and (d) UHTC at HT
511x386mm (300 x 300 DPI)

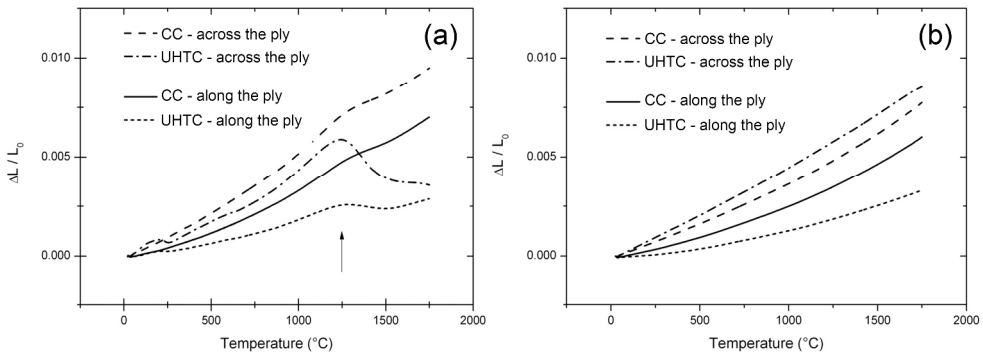

Fig 3 Change in length with temperature for CC and UHTC composites. (a) Initial run and (b) repeated run
373x136mm (300 x 300 DPI)

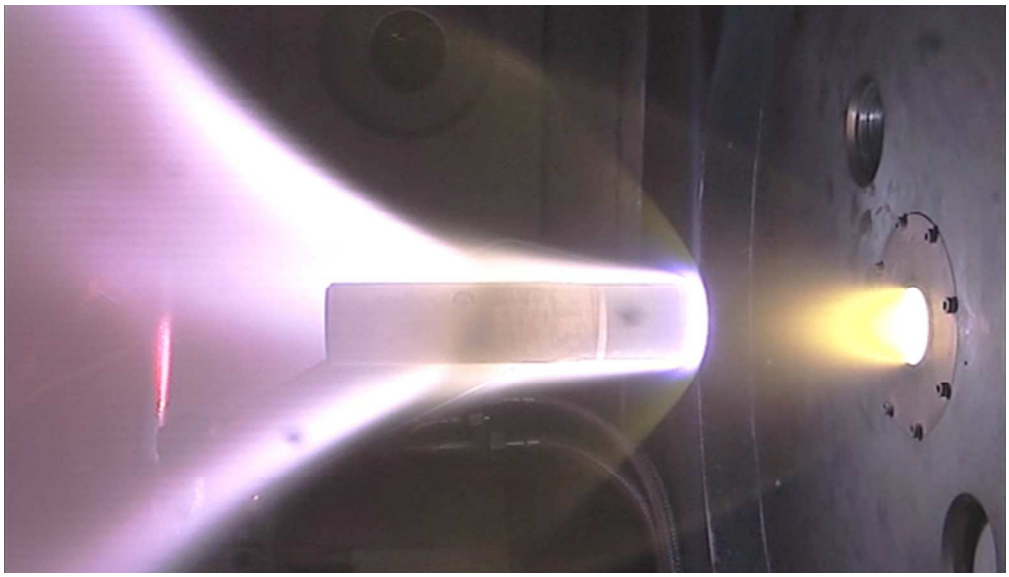

Fig 4 A picture of one of the samples being arc jet tested, showing the demanding nature of the test
82x46mm (300 x 300 DPI)

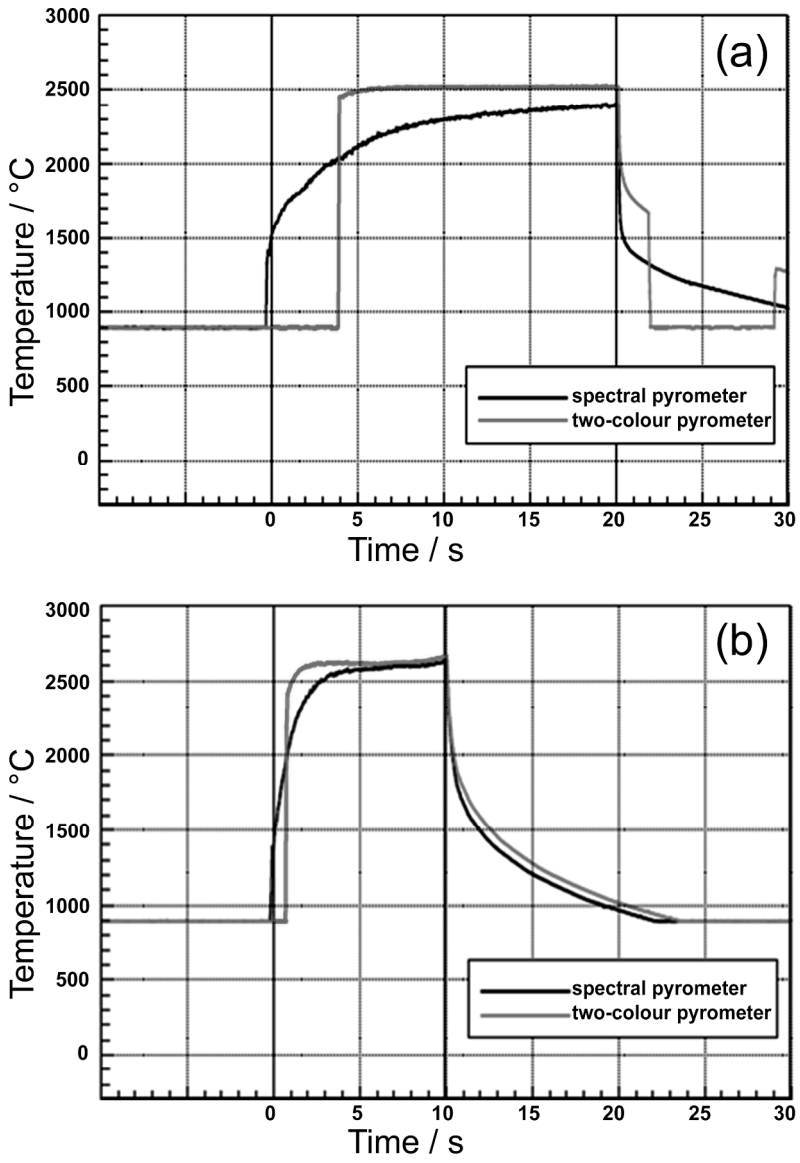

Fig 5 Time-temperature profile during the arc-jet testing of UHTC composites. (a) AJ5-20 and (b) AJ10-10
229x311mm (300 x 300 DPI)

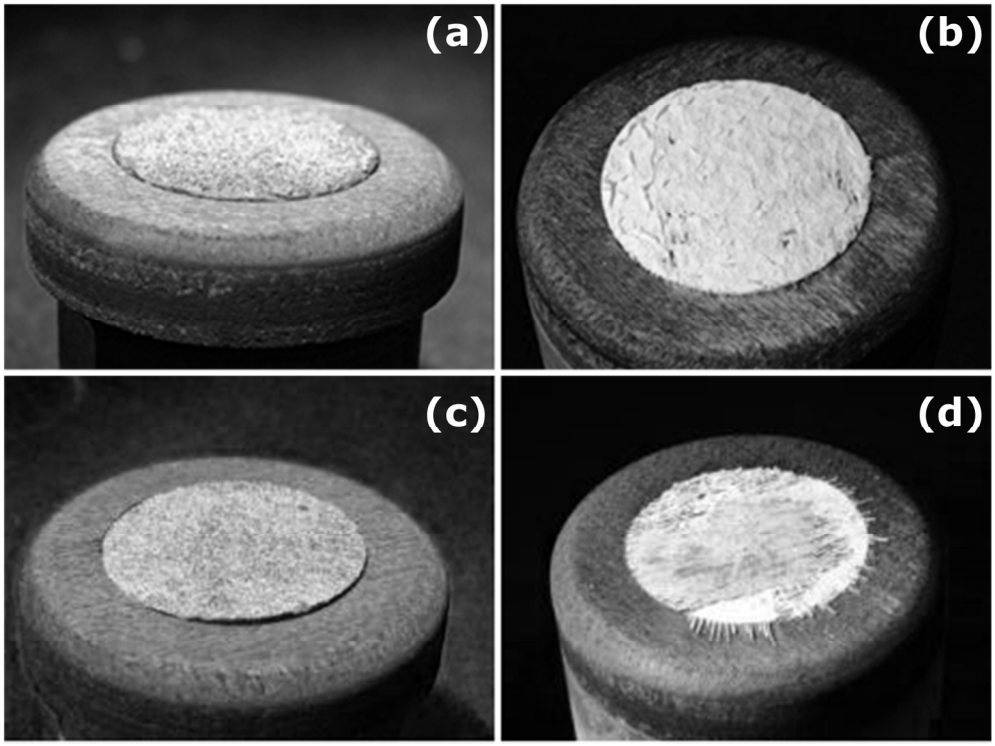

Fig 6 UHTC composites before and after arc-jet testing. (a) AJ5-20 before test, (b) AJ5-20 after test, (c) AJ10-10 before test and (d) AJ10-10 after test
164x123mm (300 x 300 DPI)

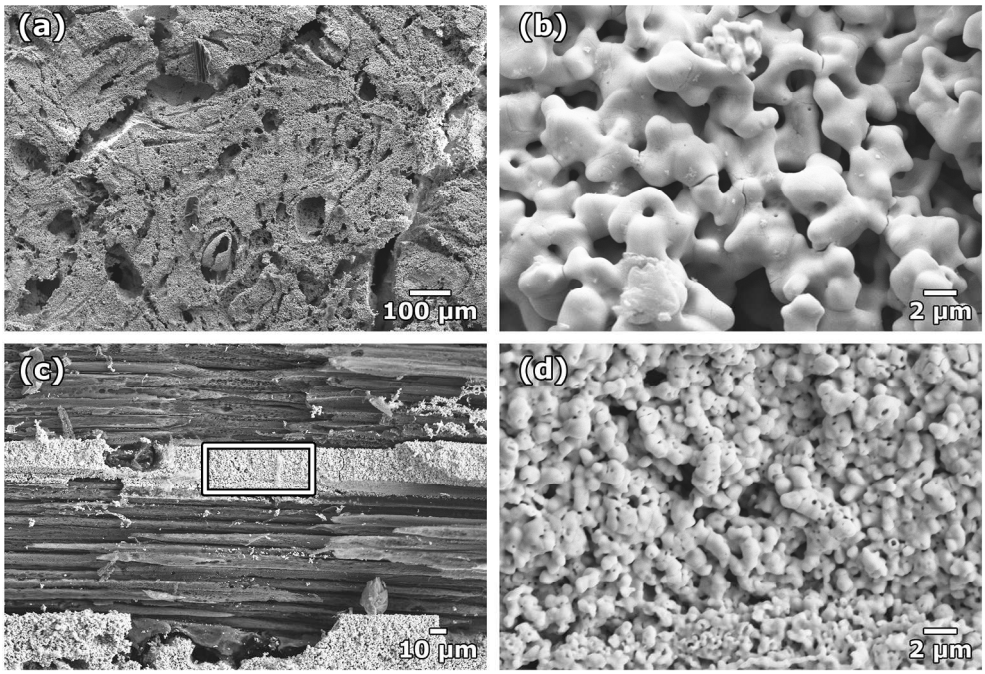

Fig 7 Surface microstructure of AJ5-20 after arc-jet testing. (a) Surface of the sample, (b) higher magnification image showing necking of oxide particles, (c) is an area where the fibres were exposed to the jet and (d) is a higher magnification image of the highlighted area showing partial oxidation of UHTC particles
199x136mm (300 x 300 DPI)

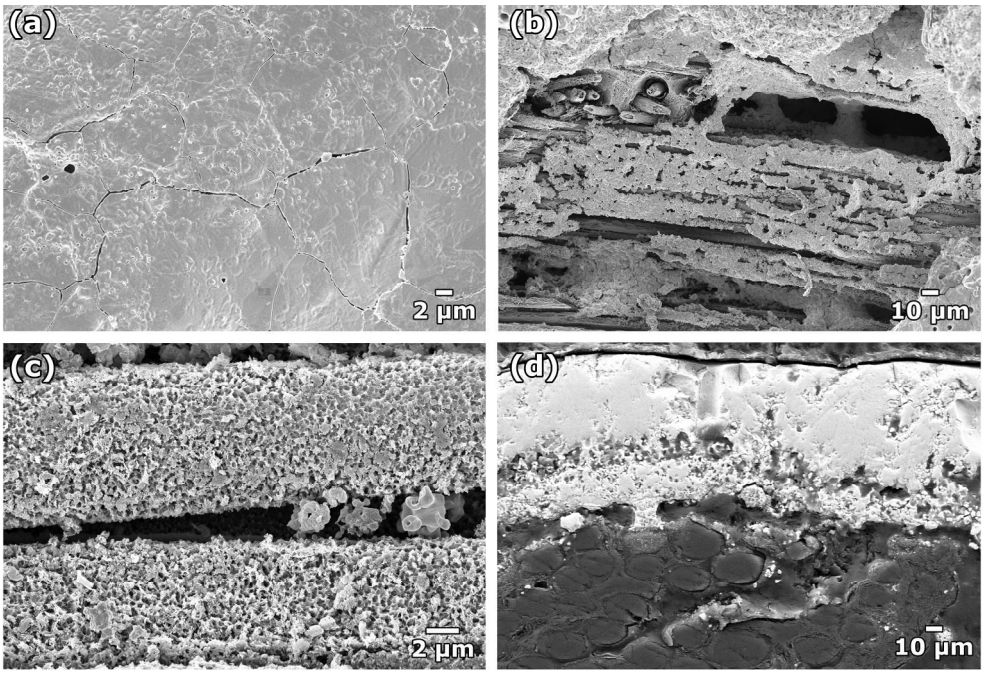

Fig 8 Microstructure of AJ10-10 after arc-jet testing. (a) Microstructure formed by the melting of UHTC particles, (b) carbon fibre protected by the UHTC phase, (c) severe pitting of fibres near the edge of the composite and (d) a cross-section revealing the thickness of the surface layer
199x136mm (300 x 300 DPI)